PAPER • **OPEN ACCESS**

Identification of tissue and therapy parameters from surface temperature.

To cite this article: Antoni Bancells Fernández 2023 *J. Phys.: Conf. Ser.* **2444** 012015

Identification of tissue and therapy parameters from surface temperature.

Antoni Bancells Fernández

Faculty of Computer Sciences, Multimedia and Telecommunication, Universitat Oberta de Catalunya (UOC),Barcelona, Spain

E-mail: afernandezb@uoc.edu , ORCID ID:0000-0002-4522-2593

Abstract. The temperature distribution of human body tissues, when electromagnetic waves are applied, is studied with the help of the bioheat equation, which is characterised by several thermal parameters, such as thermal conductivity, perfusion frequency or metabolic heat. There are also electromagnetic parameters, such as electrical conductivity and dielectric constant. Besides, therapy parameters, such as the applied power should be considered. If the values of all these parameters are known, the time evolution of the temperature can be determined. Some of these values can be found in specialised databases, and others are unknown but approximate values can be obtained by reasonable estimations. The outcome of simulations depends heavily on the parameter values. Surface temperature helps in providing better estimates of the parameter values. Once these parameters are identified, medical analyses can be performed to assess the dosimetry of the radiation so that it does not damage tissues, for example. The surface temperature is obtained from a sequence of thermographic images. Based on these experimental data, an algorithm is applied to find the values of the needed parameters. The model is simulated iteratively, adjusting the parameters at each step, reducing the approximation error between the simulation and the data. This is an optimization problem that belongs to the realm of inverse problems. It can be solved using techniques based on the gradient concept, however, this problem can be ill-conditioned, so probabilistic or evolutionary algorithms are also used. In this paper, the simulation is made using a method based on Legendre wavelets. It is proposed that the subsequent optimization is made using an evolutionary algorithm, that has shown great robustness in the problems where it has been applied. As far as known, it has never been applied to the bioheat equation. This is the aim of this work.

Keywords: bioheat equation, invers problem, Legendre wavelets, Evolutionary Centers Algorithm

1. INTRODUCTION

The knowledge of the distribution of temperatures inside the human body allows to evaluate the effect of a physical therapy on the internal tissues or find the appropriate dose so that no tissue is damaged. There are different mathematical models to know this distribution of temperatures. Some of them are are Pennes equation [1], the Cattaneo-Vernotte equation [2] [3] and the dual-phase lag equation [4]. All of them incorporate several parameters that represent the different physical processes involved.

The most common is the realization of simulations with typical values of these parameters, coming from small samples, obtained in some cases, from animal studies. For this reason, the available values show great variability, so that the results obtained are not reliable. In addition, the parameters also show variability between the individuals under study. In order to find better values, adapted to different individuals, it is necessary to carry out temperature measurements on the skin surface. Currently, high-resolution thermographic cameras are available, which are well suited for these measurements.

Additionally, their image analysis software allows recording curves of temperature evolution with respect to time. This is the data to be processed. This work has been developed in several phases:

- In first place, the different physical processes involved have been analyzed and the governing equations have been derived, based on Pennes equation [1].
- The partial differential equations have been converted into a system of ordinary differential equations through finite differences approximation for partial derivatives.
- Since the stimulus used is discontinuous in time, a resolution method known as Legendre Wavelets is used. Numerous applied examples of this technique have been found in the literature ([17], [18], [19], [20] and [21]), which have been useful for developing tools.
- Finally, the surface temperature calculated from this method allows us to find the optimal values of the parameters.

Different methods of performing this optimization have been found in the literature, which have been applied to the bioheat equation. Some of them are based on the derivative concept, for example Conjugate Gradient [5] and Levenberg-Marquardt [6]. Other methods are of the random or evolutionary type, which have greater robustness in ill-conditioned problems: Simulated Annealing [7], Markov Chain Monte Carlo [8], Genetic Algorithm [9]. In this work the use of an evolutionary algorithm, Evolutionary Centers Algorithm (ECA) method is proposed [24]. As far as it has could be known, this algorithm has not been applied to bioheat equation yet. In order to test this method, an artificial dataset has been created, simulating the system and adding Gaussian noise. The ECA method has been applied to identify the parameters. The differences between the original values of the parameters and the estimates obtained with this technique are not significant.

2. EXPERIMENTAL DATA

2.1. Diathermy device

The diathermy device is used in physical therapy in order to apply heat to the tissues, mainly to the musculoskeletal system. Its operation is based on the different electrical conductivities of the tissues when they are crossed by radio frequency waves. Essentially, a diathermy device is a UHF wave generator, with these clearly differentiated blocks: signal generator, power amplification, antenna and display. The signal generator is an FM modulator with a carrier frequency of 433 Mhz. Since this wave is not enough powerful to produce the desired therapeutic effects, it is necessary to amplify it up to a power of about 100 W. This is the signal that will be delivered to the antenna. which is a modified half dipole antenna, so it has a total length of $L = \lambda/2 = 75$ cm. This antenna is inside a header. Inside this header there is also a reflector element, which is a metal plate that concentrates the electromagnetic energy towards the therapy area. The therapy distance is about 10 cm from the center of the antenna, which is equivalent to about 5 cm from the surface of the header. Although the antenna works in the near field zone (distance less than or similar to λ), the equations of the dipole antenna in the far field (distance much greater than λ) provide relatively simple formulas that allow an estimation reasonable of the applied fields. It is also worth mentioning that, despite being a dipole antenna, it has a slightly modified geometry at its ends that does not affect the basic operation described here.

The antenna is considered to be aligned with the Z axis, and its center coincides with $z = 0$. It is fed with a current intensity $I(z)$ given by the expression (see figure 1.a):

$$I(z) = \begin{cases} I_m \cdot \cos\left(\frac{2\pi z}{\lambda}\right) & -\frac{\lambda}{4} \leq z \leq \frac{\lambda}{4} \text{ s} \\ 0 & \text{otherwise} \end{cases} \tag{1}$$

If spherical coordinates (r, ϕ, θ) and azimuth symmetry (independence with respect to ϕ) are considered (see figure 1 .b), the electric field of radiation can be expressed (see [10]):

$$\vec{E}(\theta) = E_\theta \hat{\theta} = \frac{j120e^{-j\frac{2\pi r}{\lambda}}}{r} I_m \frac{\cos(\frac{\pi}{2}\cos\theta)}{\sin\theta}\hat{\theta} \tag{2}$$

And the power density is given by:

$$P(\theta) = \frac{120 I_m^2}{\pi r^2} \left(\frac{\cos(\frac{\pi}{2}\cos\theta)}{\sin\theta} \right)^2 \tag{3}$$

where the presence of the reflector inside the header has been taken into account, with a factor of 2 in the electric field and a factor of 4 in the power density (*Image Method*).

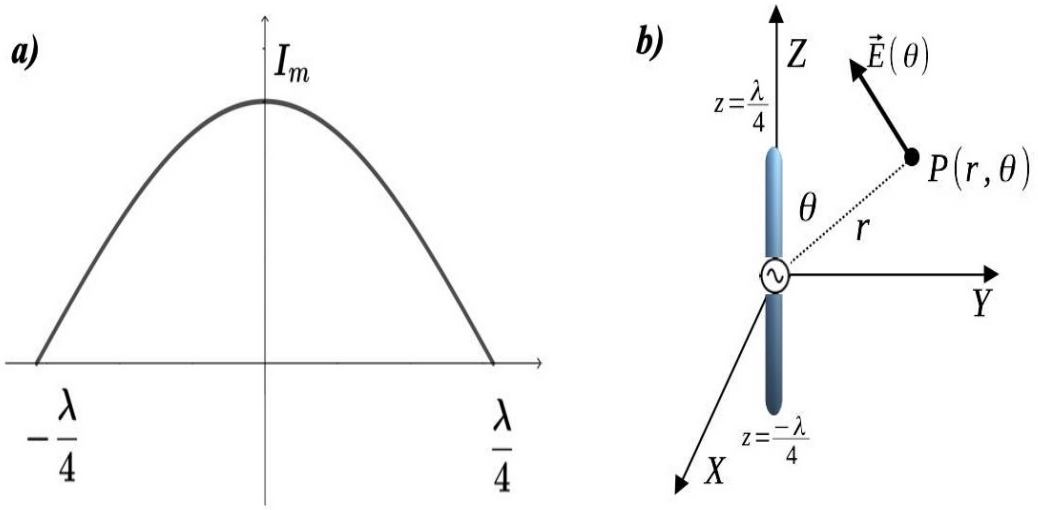

Figure 1. Antenna analysis:a) antenna current distribution; b) spherical coordinates.

As mentioned above, the header distance is $r = R = 10$ cm with a polar angle of $\theta = 90^o$, because this position gives the maximum magnitude for the electric field. Under these assumptions, the following expressions are obtained

$$E_{max} = |\vec{E}(\theta)| = \frac{120 I_m}{R} = 1200 I_m \ \frac{\text{V}}{\text{m}} \tag{4}$$

$$P(\theta) = \frac{120 I_m^2}{\pi R^2} = 3.82 \cdot 10^3 I_m^2 \ \frac{\text{W}}{\text{m}^2} \tag{5}$$

The current intensity I_m depends on the power delivered to the antenna by the electronics of the diathermy device, which can have a value up to $P_{max} = 100$ W. If the situation is represented by a one-in-one mesh electrical circuit, the signal generation is an alternating voltage source V_g ($f = 433$ MHz) in series with an impedance Z_g (*Thévenin equivalent*). The antenna is represented as a radiation impedance $Z_r \approx 75\ \Omega$. The mesh current is I_m. From this intensity it is easy to find the power delivered to the antenna or radiated power P_{max}, from where it can be solved for I_m and, consequently, E_{max} can be estimated:

$$P_{max} = Z_r I_m^2 \rightarrow I_m = \sqrt{\frac{P_{max}}{Z_r}} \rightarrow E_{max} = 1200 \cdot \sqrt{\frac{100\ \text{W}}{75\ \Omega}} \approx 1400 \ \frac{\text{V}}{\text{m}} \tag{6}$$

When the electromagnetic wave has left the antenna, it propagates through the air until it reaches the surface of the skin in the area where the therapy is applied. It is a change of material, as the wave coming from the air penetrates into a human tissue (dermis). Therefore, there is a process of reflection/refraction of electromagnetic waves that will be considered later.

2.2. Measurement process

A thermal imaging sequence of one knee has been digitized, at an image rate of every 5 seconds, for 20 minutes. A **FLIR T6600** camera was used. Diathermy therapy was applied for the first 10 minutes, to visualize the process of warming of the region of interest. The diathermy device was then

removed for the remaining 10 minutes, so that the return to steady state can be studied. In fact, this electromagnetic wave can be modeled by a discontinuous electric field $\vec{E}(\vec{r},t)$, which can be expressed as follows ($\omega = 2\pi f = 2\pi \cdot 4.33 \cdot 10^8$ rad/s $= 2.72 \cdot 10^9$ rad/s):

$$\vec{E}(\vec{r},t) = \begin{cases} \vec{E}_o(\vec{r})\cos(\omega t) & 0 \leq t \leq 600 \text{ s} \\ 0 & 600 \text{ s} \leq \text{t} \leq 1200 \text{ s} \ \vee \ \text{t} \leq 0 \end{cases} \tag{7}$$

The following measurement elements have been defined, which can be seen in Figure 2:

- Therapy measurements: El1, El4 and Bx1 are showing the process of warming/cooling.
- Control measurements: El2 and El3 are giving the evolution of the basal temperature of the patient throughout the process

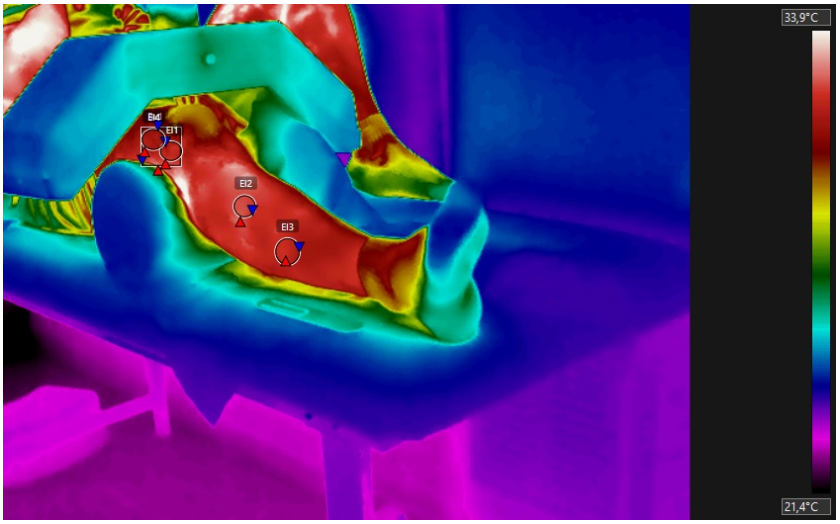

Figure 2. Measurements in the thermographic sequence.

2.3. Evolution of surface temperature over time

It can be seen, in Figure 3, the mean values of all these measurements plotted over time. It is important to note here that the camera was turned on one minute before the diathermy treatment device was turned on and then the described experiment was performed. This is the reason why during the first 60 seconds the system stays in the basal state, goes up to 660 seconds and goes down again between 660 and 1260 seconds. In other words, it has a gap of 60 s.

Control measures El2 and El3 have average values of 32.0 ^{o}C and 32.6 ^{o}C, respectively, both with standard deviation $s = 0.13$ ^{o}C. However, therapy measures behave very differently. Initially, they show a certain inertia to change with respect to their basal value, approximately 32 ^{o}C, for the first minute. After this time, they increase significantly in the next 4 minutes. This growth is reduced for the next 5 minutes, until the diathermy device is removed. After 10 minutes the temperature drops, returning to the steady state, that is, to the basal state, but slower than the rise. For example, if a linear fit is made for Bx1, with data between 60 s and 300 s, the following expression is obtained:

$$T = 1.602 \cdot 10^{-2}(t - 60) + 32.176 \tag{8}$$

where T is the temperature in ^{o}C and t is time in seconds. The correlation coefficient is $r = 0.9984$. It means, for this example, that the temperature is increased by 0.016 ^{o}C/s $= 0.96$ ^{o}C/min ≈ 1 ^{o}C/min. Then, after that, the mechanism of regulating body temperature is slowing growth. If it did not exist, the temperature would rise indefinitely and tissues would burn.

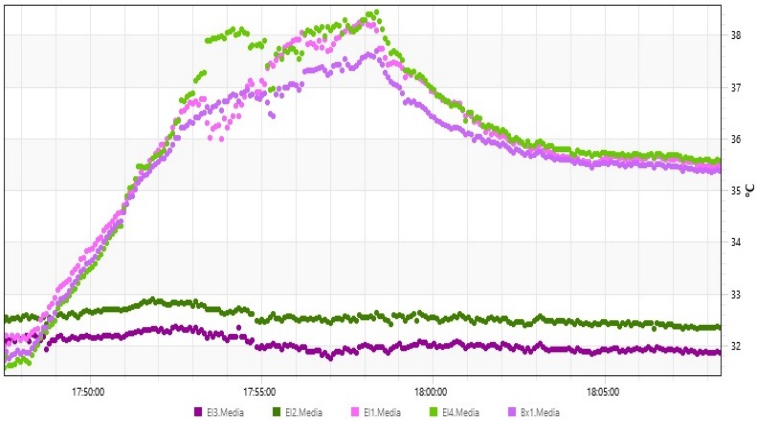

Figure 3. Evolution of temperature measurements.

3. MATHEMATICAL MODEL

3.1. Bioheat equation and boundary conditions

The simplest model for temperature evolution inside a tissue is obtained by energy balance. Without loss of generality, the one-dimensional form is considered here. The basic idea is that the power per unit volume is obtained by adding different terms:

$$\rho c \frac{\partial T}{\partial t} = \sum_i q_i(z,t) \tag{9}$$

where ρ is the density of tissue and c is its specific heat. Positive terms correspond to warming, while negative terms correspond to cooling. All terms that have physical interest are considered below. The first of these is the diffusion term, which is represented by. According to the Fourier law , the heat flux that is transferred by diffusion fulfills the relationship:

$$Q = -k \frac{\partial T}{\partial z} \tag{10}$$

where k is the thermal conductivity of tissue. Therefore, the power per unit volume due to the diffusion can be expressed as follows:

$$q_d(z,t) = \frac{-\partial Q}{\partial z} = \frac{-\partial \left(-k \frac{\partial T}{\partial z}\right)}{\partial z} = k \frac{\partial^2 T}{\partial z^2} \tag{11}$$

On the other hand, there is internal heat generation due to metabolism, which is represented by $q_m(z,t)$, which can be considered uniform and constant throughout the tissue, so it can be written:

$$q_m(z,t) = A_o \tag{12}$$

If an electric field $\vec{E}$ is externally applied, another term $q_e(z,t)$ must be added, and can be expressed:

$$q_e(z,t) = \frac{\sigma |\vec{E}|^2}{2} \tag{13}$$

This field $\vec{E}$ depends on the electrical permittivity ε and the electrical conductivity σ. It will be explained in more depth below.

Finally, the cooling effect of the blood circulation is considered. In the first approximation it is assumed a form similar to the Newton Law :

$$q_b(z,t) = \rho_b c_b \omega_b (T_b - T) \tag{14}$$

where ω_b is the blood perfusion frequency, ρ_b its density, c_b its specific heat, and T_b its temperature. The product of the first three values is called the blood perfusion coefficient b:

$$b = \rho_b c_b \omega_b \tag{15}$$

ρ, c, k, b and A_o are known as **thermophysical tissue parameters**, whereas ε_r and σ are the **electrical tissue parameters**.

With all these assumptions, energy balance equation (9) can be written as

$$\rho c \frac{\partial T}{\partial t} = q_d(z,t) + q_m(z,t) + q_e(z,t) + q_b(z,t) \tag{16}$$

If equations from (11) to (14) are substituted into the before equation, it is obtained the **Bioheat equation**:

$$\rho c \frac{\partial T}{\partial t} = k \frac{\partial^2 T}{\partial z^2} + b(T_b - T) + A_o + \frac{\sigma |\vec{E}|^2}{2} \tag{17}$$

In order to express this equation in a more compact form, it is divides the entire equation by ρc and the following magnitudes are defined:

$$\tau = \frac{\rho c}{b} \quad , \quad \alpha = \frac{k}{\rho c} \quad , \quad q(z,t) = A_o + \frac{\sigma |\vec{E}|^2}{2} \tag{18}$$

This is the form of the Bioheat equation with which it has been working:

$$\frac{\partial T}{\partial t} = \alpha \frac{\partial^2 T}{\partial z^2} + \frac{T_b - T}{\tau} + \frac{q(z,t)}{\rho c} \tag{19}$$

In the basal state (absence of electromagnetic energy), tissue is in steady state , so It can be written:

$$\frac{\partial T}{\partial t} = 0 \tag{20}$$

and the Bioheat equation is becoming an ordinary differential equation:

$$\alpha \frac{\partial^2 T_0}{\partial z^2} + \frac{T_b - T_0}{\tau} + \frac{A_o}{\rho c} = 0 \tag{21}$$

where $T_o(z)$ is the solution of the above equation, and which has a relatively easy analytical solution to find from the boundary conditions seen below. It is the temperature at which the tissue is per $t < 0$. In addition, it is the initial condition for the next phase, i.e.:

$$T(z,0) = T_0(z) \tag{22}$$

Once the initial condition has been considered, the boundary conditions need to be defined. First of all, at $z = 0$ which is the border of tissue with outside, a convection heat transfer occurs, that is given by the equation:

$$-k \frac{\partial T(0,t)}{\partial z} = h(T_a - T(0,t)) \tag{23}$$

where h is the **convection heat transfer coefficient** and T_a is the external temperature. For convenience, It is defined $B = \frac{h}{k}$, so this equation is converted in:

$$\frac{\partial T(0,t)}{\partial z} = -B(T_a - T(0,t)) \tag{24}$$

Similarly, at $z = L$, which is the deeper part of tissue, assuming it is thick enough, it is well suited for the adiabatic condition:

$$\frac{\partial T(L,t)}{\partial z} = 0 \tag{25}$$

3.2. Tissue parameters and electromagnetic model

Tissue parameters and electromagnetic model are available from an online database for human tissue parameters from IT'IS Foundation,a non-profit organization dependent from the Swiss Federal Institute of Technology (ETH) at Zurich [12]. Some of the typical values of thermophysical parameters estimated by several methods are shown in Table 1 [16]. It is also important to give the value of the convective heat transfer coefficient h and the external temperature T are 10 $\frac{\mathrm{W}}{^{o}\mathrm{C}\cdot\mathrm{m}^2}$ and 23.7 ^{o}C respectively.

Table 1. Representative thermal parameters values

Tissue	$c(\frac{\mathrm{J}}{\mathrm{C}\cdot\mathrm{kg}})$	$k(\frac{\mathrm{W}}{^{o}\mathrm{C}\cdot\mathrm{m}})$	$\rho(\frac{\mathrm{kg}}{\mathrm{m}^3})$	$b(\frac{\mathrm{W}\cdot^{o}\mathrm{C}}{\mathrm{m}^3})$	$\tau(\mathrm{s})$	$\alpha(\frac{\mathrm{m}^2}{\mathrm{s}})$	$A_o(\frac{\mathrm{W}}{\mathrm{m}^3})$
Blood vessel	3651	0.51	1046	-	-	$1.34 \cdot 10^{-7}$	488
Bone-cancellous	2292	0.29	1210	932	2976	$1.05 \cdot 10^{-7}$	227
Bone-cortical	1244	0.30	932	-	-	$1.32 \cdot 10^{-7}$	0
Cartilage	3354	0.50	1099	2429	1518	$1.36 \cdot 10^{-7}$	591
Fat	2065	0.21	909	1626	1154	$1.12 \cdot 10^{-7}$	395
Ligaments/tendons	3364	0.44	1174	2161	1828	$1.11 \cdot 10^{-7}$	526
Muscle-skeletal	3322	0.49	1103	1930	1899	$1.34 \cdot 10^{-7}$	748
Skin	3250	0.43	1114	3687	982	$1.19 \cdot 10^{-7}$	452

Next, the electromagnetic term is considered in depth. Revision of Maxwell's equations is necessary. Maxwell equations for isotropic non-magnetic lossy material with conductivity σ and relative dielectric permittivity ε_r are considered [11]. If sinusoidal and planar waves are considered, with electric field oriented over X direction and magnetic field oriented over Y direction, and after making some calculations, **wave equations** are obtained:

$$\frac{\partial^2 E_x}{\partial z^2} = \gamma^2 E_x \quad , \quad \frac{\partial^2 H_y}{\partial z^2} = \gamma^2 H_y \tag{26}$$

where γ is the **propagation constant** and $\gamma^2 = -\omega^2 \mu_o \varepsilon_r \varepsilon_o (1 - j \tan\delta)$ and δ is the **loss angle**. The solution of the equation 26) can be expressed in closed form as

$$E_x = E_+ e^{-\gamma z} + E_- e^{\gamma z} \quad , \quad H_y = \frac{-j\gamma}{\omega \mu_o}(E_+ e^{-\gamma z} - E_- e^{\gamma z}) \tag{27}$$

The first term of the equation (27), that is $E_+ e^{-\gamma z}$, is known as **progressive wave** because it represents a wave which is traveling towards positive z. Conversely, the second term is known as **regressive** wave because it's a wave that travels in the opposite direction. If there are only progressive waves and electric field is divided by magnetic field, it is obtained the **characteristic impedance** for this material. Its expression is:

$$\eta = \frac{j\omega\mu_o}{\gamma} \tag{28}$$

Once the expressions for both electric and magnetic fields are available, it can be defined the **power density** vector, known also as Poynting vector, defined as:

$$\vec{P} = \frac{Re(\vec{E} \times \vec{H}^*)}{2} \tag{29}$$

Electromagnetic heating of tissues Q_e can be quantified as the rate of reduction for the module of the power density vector P, which is expressed mathematically as a derivative of P over z, with a change of sign:

$$Q_e = -\frac{dP}{dz} \tag{30}$$

It can be shown that

$$Q_e = \frac{\vec{J} \cdot \vec{E}}{2} = \frac{\sigma |\vec{E}|^2}{2} \tag{31}$$

Real human body has several discontinuities or material changes. Let's consider that at $z = z_i$ there are two different tissues with parameters γ_i and η_i at left, and γ_{i+1} and η_{i+1} at right. Electric and magnetic fields must be continuous:

$$E_x(z_i^-) = E_x(z_i^+) \quad , \quad H_y(z_i^-) = H_y(z_i^+) \tag{32}$$

Each slab of tissue can be viewed like a piece of transmission line, as you can see in the figure 4. For example, in the first place is **skin**, with length l_s and parameters η_s and γ_s. After, follows **fat**, with length l_f and parameters η_f and γ_f. Next, it is **muscle**, with length l_m, and parameters η_m and γ_m. Finally, it is **bone**, width length l_b, and parameters η_b and γ_b. As it can be seen in the figure (4), the positions of their lower ends are, respectively, z_s, z_f,z_m and $z_b = L$.

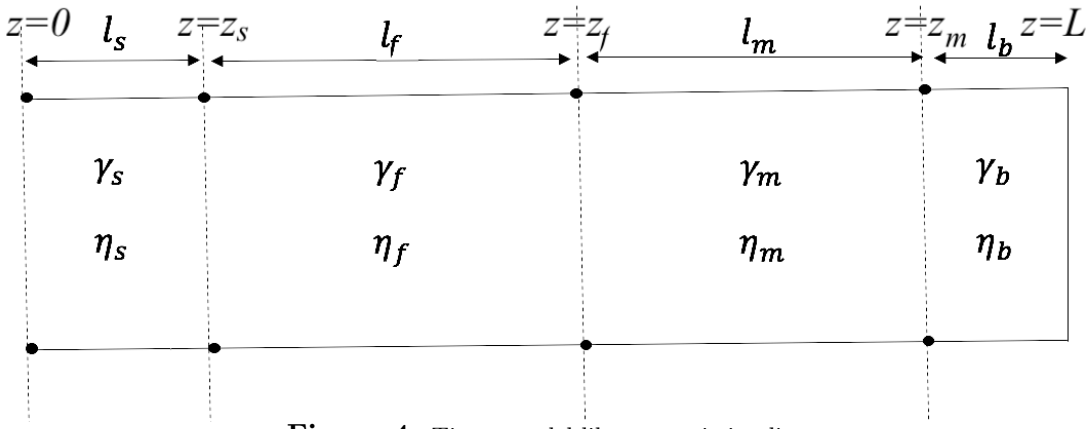

Figure 4. Tissue model like transmission line

It could be applied (32) at each discontinuity to get an equation system, but it's better to work with impedance and reflection coefficients. Let's consider a tissue discontinuity at point $z = z_i$. At left ($z < z_i$) there is the tissue i, with a propagation constant γ_i and characteristic impedance η_i, whereas at right ($z > z_i$) there is another tissue $i + 1$, with propagation constant and characteristic impedance γ_{i+1} and characteristic impedance η_{i+1}, respectively. Let's begin with left tissue. The electric field $E_x(z)$ can be expressed as follows:

$$E_x(z) = E_i^+ e^{-\gamma_i z} + E_i^- e^{\gamma_i z} \tag{33}$$

If common factor is taken, we have:

$$E_x(z) = E_i^+ \left(e^{-\gamma_i z} + \frac{E_i^-}{E_i^+} e^{-\gamma_i z} \right) = E_i^+ (e^{-\gamma_i z} + \rho_i e^{\gamma_i z}) \tag{34}$$

where ρ_i is the **reflection coefficient**, defined as follows:

$$\rho_i = \frac{E_i^-}{E_i^+} \tag{35}$$

As for the magnetic field, It is expressed:

$$H_y(z) = \frac{E_i^+}{\eta_i} (e^{-\gamma_i z} - \rho_i e^{\gamma_i z}) \tag{36}$$

The **Impedance** function is defined as is defined as the quotient between the electric field E_x and the magnetic field H_y. Its expression is:

$$Z_i(z) = \eta_i \left(\frac{e^{-\gamma_i z} + \rho_i e^{\gamma_i z}}{e^{-\gamma_i z} - \rho_i e^{\gamma_i z}} \right) = \eta_i \left(\frac{1 + \rho_i e^{2\gamma_i z}}{1 - \rho_i e^{2\gamma_i z}} \right) \tag{37}$$

Similarly, for the tissue $i+1$ its expression is:

$$Z_{i+1}(z) = \eta_{i+1}\left(\frac{1+\rho_{i+1}e^{2\gamma_{i+1}z}}{1-\rho_{i+1}e^{2\gamma_{i+1}z}}\right) \tag{38}$$

This function must be continuous at point $z = z_i$, so it can be written

$$Z_i(z_i^-) = Z_{i+1}(z_i^+) \tag{39}$$

Taking it into account equations (37), It can be solved for ρ_i:

$$\eta_i\left(\frac{1+\rho_i e^{2\gamma_i z_i}}{1-\rho_i e^{2\gamma_i z_i}}\right) = Z_{i+1}(z_i^+) = Z_{i+1} \rightarrow \rho_i = \left(\frac{Z_{i+1}-\eta_i}{Z_{i+1}+\eta_i}\right)e^{-2\gamma_i z_i} \tag{40}$$

These equations were applied to the electromagnetic model. Equations (38) and (40) were applied successively to each tissue change, starting at the bottom, where $\rho_b = -1$ is assumed (there isn't dissipated power). Once the reflection coefficients at each discontinuity, the incident electric fields E_i^+ can be calculated. The electric field E_a^+ delivered by the antenna must be estimated based on its physical characteristics. E_s^+, E_f^+, E_m^+, E_b^+ are obtained from the equation (32). Once these fields are obtained, the electric field $E_x(z)$ can be expressed as follows:

$$E_x(z) = \begin{cases} E_s^+(e^{-\gamma_s z} + \rho_s e^{\gamma_s z}) & 0 \le z \le z_s \\ E_f^+(e^{-\gamma_f z} + \rho_f e^{\gamma_f z}) & z_s \le z \le z_f \\ E_m^+(e^{-\gamma_m z} + \rho_m e^{\gamma_m z}) & z_f \le z \le z_m \\ E_b^+(e^{-\gamma_b z} - e^{\gamma_b z}) & z_m \le z \le L \end{cases} \tag{41}$$

As an application, numerical values have been given to the example to perform a simulation:

- Skin $l_s = 1.60 \cdot 10^{-3}$ m $= 1.6$ mm
- Fat $l_f = 1.44 \cdot 10^{-2}$ m $= 1.44$ cm
- Muscle $l_m = 2.00 \cdot 10^{-2}$ m $= 2.00$ cm
- Bone $l_b = 4.00 \cdot 10^{-3}$ m $= 4.00$ mm

The electromagnetic properties that have been taken into account can be seen in table (2). It has been added propagation constant γ and characteristic impedance η.

Table 2. Electromagnetic properties for the example ($f = 433$Mhz)

Tissue	ϵ_r	σ $(\Omega^{-1}\cdot \mathrm{m}^{-1})$	γ (m^{-1})	η (Ω)
Air	1	0	$9.09j$	377
Skin	46.1	0.702	$18.7 + 64.5j$	$49.0 + 14.2j$
Fat	11.6	$8.22 \cdot 10^{-2}$	$4.50 + 31.3j$	$107.3 + 15.4j$
Muscle	56.9	0.805	$19.4 + 71.2j$	$44.8 + 12.2j$
Bone	22.3	0.241	$4.86 + 33.3j$	$100.9 + 14.7j$

In a previous section it has been seen that the electric field coming from the antenna has a magnitude $E_d = 1386 \frac{\mathrm{V}}{\mathrm{m}} \approx 1400 \frac{\mathrm{V}}{\mathrm{m}}$. Reflection coefficient ρ_i and incident electric field E_i^+ are summarized at table (3). It has been calculated the electric field E_x and the magnetic field H_y as a function of depth, shown at figure 5. Both are continuous functions, but electric field is an increasing function with a maximum value $E_{max} = 405 \frac{\mathrm{V}}{\mathrm{m}}$ at surface. It has been calculated also the electromagnetic heating Q_e as a function of depth. It is observed (figure 6.a) that is a discontinuous function because electrical conductivity is also discontinuous . It has important values in two areas, which correspond to the skin and muscle tissue, because these tissues are more conductive than others. In order to make this graph more meaningful, its value has been divided by the factor ρc for each tissue (figure 6.b), where ρ is the tissue density and c is its specific heat. It gives the rate of temperature increase as a function of time. At the surface, it gives 0.016 ^{o}C/s, which is consistent with experimental data.

Table 3. Reflection coefficient and incident electric field

Tissue	**Reflection coefficient** ρ_i	**Incident electric field** E_i^+ $(\frac{\mathrm{V}}{\mathrm{m}})$
Air	$\rho_a = -0.463 - 0.413j$	$E_a^+ = -194.5 - 1048.7j$
Skin	$\rho_s = -0.009 - 1.35j$	$E_s^+ = -117.4 + 1204.1j$
Fat	$\rho_f = 0.075 - 0.036j$	$E_f^+ = -328.9 - 182.7j$
Muscle	$\rho_m = -1.01 - 0.01j$	$E_m^+ = -167.8 + 78.8j$
Bone	$\rho_b = -1$	$E_b^+ = -341.8 + 203.4j$

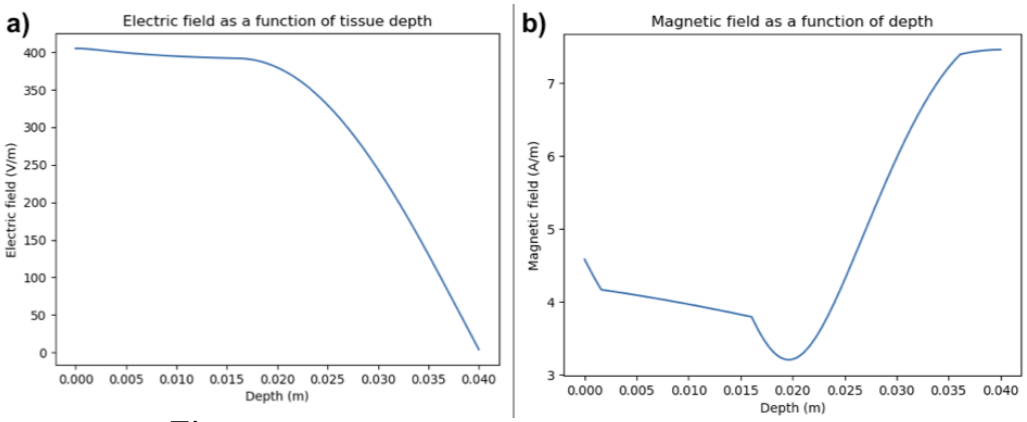

Figure 5. Electric and magnetic fields as a function of depth.

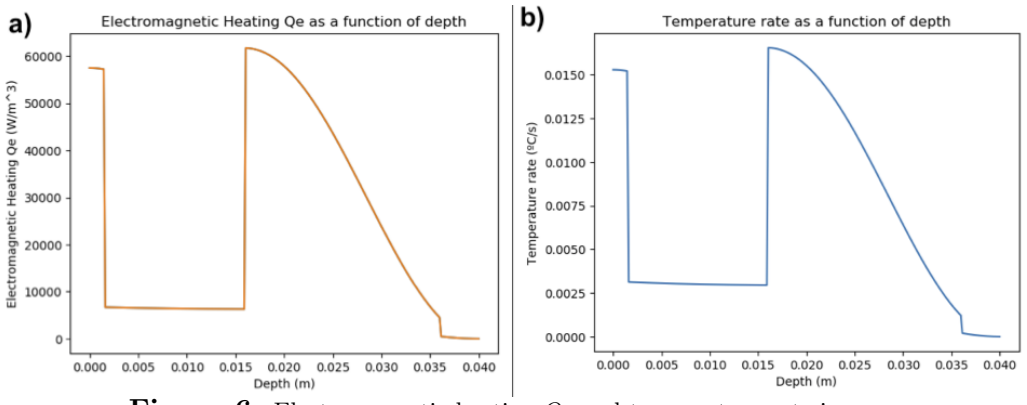

Figure 6. Electromagnetic heating Q_e and temperature rate increase

4. DIRECT PROBLEM SOLUTION

This section explains how to find the solution of the proposed mathematical model with typical values of its parameters, which are found in databases or in the literature. This is called **Direct Problem**. Once the solution $T(z,t)$ is obtained, the surface temperature $T(0,t)$ is calculated, which will then be compared with the information obtained from the thermographic camera. The process started with the basal state, which gives the initial conditions, and then see how to calculate the temperature at any later time.

4.1. Basal state solution

Since the basal state provides the initial conditions of the problem, the first step that will be taken is to determine it. If single-tissue model is considered, i.e., equation (21), with its boundary conditions (24) and (25) with $t = 0$, It has analytical solution, since A_o does not depend on z, so this boundary problem can be studied as an ordinary differential equation with constant coefficients. Its solution has this form:

$$T_o(z) = T_b + \frac{A_o\tau}{\rho c} + C\sinh(\frac{z-L}{\sqrt{\alpha\tau}}) + D\cosh(\frac{z-L}{\sqrt{\alpha\tau}}) \tag{42}$$

The boundary condition at $z = L$ implies that $C = 0$. The boundary condition at $z = 0$ let to find the value of D, which results:

$$D = \frac{B(T_a - T_b - \frac{A_o\tau}{\rho c})}{B\cosh(\frac{L}{\sqrt{\alpha\tau}}) + \frac{1}{\sqrt{\alpha\tau}}\sinh(\frac{L}{\sqrt{\alpha\tau}})} \tag{43}$$

$To(0)$ can be calculated substituting the before equation into equation (42) and taking $z = 0$. The result is given by the formula:

$$T_o(0) = T_b + \frac{A_o\tau}{\rho c} + \frac{B(T_a - T_b - \frac{A_o\tau}{\rho c})}{B\cosh(\frac{L}{\sqrt{\alpha\tau}}) + \frac{1}{\sqrt{\alpha\tau}}\sinh(\frac{L}{\sqrt{\alpha\tau}})}\cosh(\frac{L}{\sqrt{\alpha\tau}}) \tag{44}$$

4.2. Model discretization

The next step is to solve the problem for $t > 0$. In order to make the explanation simpler , single-tissue model is considered. Previous to discretization, terms in equation (19) must be grouped. If it is defined the expression:

$$\Theta(z,t) = \frac{\rho c T_b}{\tau} + A_o + \frac{\sigma|\vec{E}(z,t)|^2}{2} \tag{45}$$

then equation (19) is transformed as follows:

$$\frac{\partial T(z,t)}{\partial t} = \alpha\frac{\partial^2 T(z,t)}{\partial z^2} - \frac{T(z,t)}{\tau} + \frac{\Theta(z,t)}{\rho c} \tag{46}$$

A discretization has been performed by the finite difference method only in the part of the spatial coordinate z, with step $\Delta z = \frac{L}{N}$, but the time t has been left as a continuous variable. This discretization can be expressed as:

$$T(i\Delta z, t) = T_i(t) \tag{47}$$

where i=1,2..., N-1 are the indexes of each node. Let's discretize each term of equation (46) separately, taking in account that vector form is considered. Each term in the equation is replaced by the expression to the right of each arrow:

- $T(z,t) \to \bar{T}(t)$ column vector with N-1 components $T_i(t)$
- $\frac{\partial T(z,t)}{\partial t} \to \frac{d\bar{T}(t)}{dt}$ column vector with N-1 components $\frac{dT_i(t)}{dt}$
- $\frac{\Theta(z,t)}{\rho c} \to$ column vector with N-1 components again, but now $\Theta_i(t) = \Theta(i\Delta z, t)$, i=1,2..., N-1

The whole term $\alpha\frac{\partial^2 T(z,t)}{\partial z^2} - \frac{T(z,t)}{\tau}$ is transformed as $\bar{\bar{A}}\cdot\bar{T}(t) + \bar{\Theta}_a$, where $\bar{\bar{A}}$ is an (N-1)-order tridiagonal square matrix and $\bar{\Theta}_e$ is a column vector with N-a1 components with all zero elements except the first. Their structure are explained below. Let's see. If the second order partial derivatives are approximated by a finite differences formula:

$$\frac{\partial^2 T(i\Delta z, t)}{\partial z^2} \approx \frac{T_{i+1}(t) - 2T_i(t) + T_{i-1}(t)}{\Delta z^2} \tag{48}$$

then

$$\frac{\alpha\partial T(i\Delta z, t)}{\partial z^2} - \frac{T(i\Delta z, t)}{\tau} \approx \frac{\alpha T_{i+1}(t)}{\Delta z^2} - \left(\frac{2\alpha}{\Delta z^2} + \frac{1}{\tau}\right)T_i(t) + \frac{\alpha T_{i-1}(t)}{\Delta z^2} \tag{49}$$

These equations are correct for i=2,3..., N-2. For i=1, it is necessary an expression for $T_o(t)$, which can be derived if a finite differences approximation for $\frac{\partial T(0,t)}{\partial z}$ is considered:

$$\frac{\partial T(0,t)}{\partial z} = \frac{-3T_o(t) + 4T_1(t) - T_2(t)}{2\Delta z} \rightarrow T_0(t) = \frac{4T_1(t) + T_2(t)}{3 + 2B\Delta z} + \frac{2B\Delta z T_a}{3 + 2B\Delta z} \tag{50}$$

If equation (50) is substituted into equation (49) for $i = 1$, and after doing a bit of algebra:

$$\frac{\alpha\partial T(\Delta z,t)}{\partial z^2} - \frac{T(\Delta z,t)}{\tau} = -\left[\frac{1}{\tau} + \frac{\alpha}{\Delta z^2}\left(\frac{2+4B\Delta z}{3+2B\Delta z}\right)\right]T_1(t) + \frac{\alpha}{\Delta z^2}\left(\frac{2+2B\Delta z}{3+2B\Delta z}\right)T_2(t) + \frac{2\alpha B T_a}{(3+2B\Delta z)\Delta z} \tag{51}$$

Similarly, for i=N-1, It is necessary an expression for $T_N(t)$, which can be derived if a finite differences approximation for $\frac{\partial T(L,t)}{\partial z}$ is considered:

$$\frac{\partial T(Z,t)}{\partial z} = \frac{3T_N(t) - 4T_{N-1}(t) + T_{N-2}(t)}{2\Delta z} \rightarrow T_N(t) = \frac{4T_{N-1}(t) - T_{N-2}(t)}{3} \tag{52}$$

If equation (52) is substituted into equation (49) for i =N-1, and after doing some algebra:

$$\frac{\alpha\partial T(Z,t)}{\partial z^2} - \frac{T(Z,t)}{\tau} = \frac{2\alpha}{3\Delta z^2}T_{N-2}(t) - \left(\frac{1}{\tau} + \frac{2\alpha}{3\Delta z^2}\right)T_{N-1}(t) \tag{53}$$

In summary, these linear relationships for $\alpha\frac{\partial T}{\partial z^2} - \frac{T}{\tau}$ can be expressed in matrix form $\bar{\bar{A}} \cdot \bar{T}(t) + \bar{\Theta}_a$ as follows:

- Rows from i=2 to i=N-2:

$$a_{ij} = \begin{cases} -\left(\frac{2\alpha}{\Delta z^2} + \frac{1}{\tau}\right) & j = i \\ \frac{\alpha}{\Delta z^2} & j = i-1 \vee j = i+1 \\ 0 & \text{otherwise} \end{cases} \tag{54}$$

- Row i=1:

$$a_{1j} = \begin{cases} -\left[\frac{1}{\tau} + \frac{\alpha}{\Delta z^2}\left(\frac{2+4B\Delta z}{3+2B\Delta z}\right)\right] & j = 1 \\ \frac{\alpha}{\Delta z^2}\left(\frac{2+2B\Delta z}{3+2B\Delta z}\right) & j = 2 \\ 0 & \text{otherwise} \end{cases} \tag{55}$$

- Row i=N-1:

$$a_{N-1,j} = \begin{cases} \frac{2\alpha}{3\Delta z^2} & j = N-2 \\ -\left(\frac{1}{\tau} + \frac{2\alpha}{3\Delta z^2}\right) & j = N-1 \\ 0 & \text{otherwise} \end{cases} \tag{56}$$

$\bar{\Theta}_a$ is defined as follows:

$$\Theta_{ai} = \begin{cases} \frac{2\alpha B T_a}{(3+2B\Delta z)\Delta z} & i = 1 \\ 0 & \text{otherwise} \end{cases} \tag{57}$$

It is got a first order ordinary differential equations system , which in our case is linear. If $\Psi(t)$ is defined as:

$$\bar{\Phi}(t) = \bar{\Theta}_a + \frac{\bar{\Theta}(t)}{\rho c} \tag{58}$$

the resulting system is:

$$\frac{d\bar{T}(t)}{dt} = \bar{\bar{A}} \cdot \bar{T}(t) + \bar{\Phi}(t) \tag{59}$$

The simplest approach to solving this system is to use finite differences to discretize time derivatives (Euler method), but the most common is to apply more accurate and stable methods. In recent times, methods have been developed that are based on the possibility that the vector function to be found is a linear combination of discontinuous orthogonal functions with different degrees of resolution, called Wavelets, so that they can mathematically represent systems in which the energy supply is discontinuous over time. For example, it is the case of a heat equation with an energy source that turns on at maximum power for a certain time, say 10 min, and turns off for the remaining 10 min. If the properties of the wavelets are applied, it is possible to transform a differential equation or a system in algebraic equations whose unknowns are the coefficients by which the basis functions will be multiplied to get the solution of the differential equation. This system will be linear if the original system is linear ([17], [18], [19], [20] and [21]).

4.3. Legendre wavelets:function approximation and operational integration matrix
Let's consider a function $f(t)$ defined over the interval [0,1]. Let's build the approximation function $\hat{f}(t)$:

$$\hat{f}(t) = \sum_{n=1}^{2^{k-1}} \sum_{m=0}^{M-1} c_{mn} \psi_{mn}(t) \tag{60}$$

where the basic functions $\psi_{mn}(t)$ are Legendre polynomials of order m defined over the interval $\left[\frac{\hat{n}-1}{2^k}, \frac{\hat{n}+1}{2^k}\right]$ and $\hat{n} = 2n-1$, $n = 1, 2, 3, ..., 2k-1$, which are defined by the expression:

$$\psi_{mn}(t) = \begin{cases} \sqrt{m+\frac{1}{2}} 2^{\frac{k}{2}} P_m\left(2^k t - \hat{n}\right) & \frac{\hat{n}-1}{2^k} \leq t \leq \frac{\hat{n}+1}{2^k} \text{ s} \\ 0 & \text{otherwise} \end{cases} \tag{61}$$

The interval [0,1] is being divided into 2^{k-1} width sub-intervals $\frac{1}{2^{k-1}}$, and in each one has a base of Legendre polynomials, scaled by a factor $\sqrt{m+\frac{1}{2}} 2^{\frac{k}{2}}$ and delayed $t = \frac{\hat{n}}{2^k}$, which allows to approximate any function defined in the interval [0,1], although it could be discontinuous. If the first M polynomials of Legendre are used into each interval, The coefficients c_{mn} are calculated with the formula:

$$c_{mn} = \int_0^1 f(t) \psi_{mn}(t) dt \tag{62}$$

If the way in which the base functions have been defined is taken into account and the variable $\chi = 2^k t - (2n-1)t$ is changed, the following expression is obtained:

$$c_{mn} = \sqrt{m+\frac{1}{2}} 2^{\frac{-k}{2}} \int_{-1}^{1} f\left(\frac{\chi + 2n - 1}{2^k}\right) P_m(\chi)\, dt \tag{63}$$

The last expression is calculated with a Gauss-Legendre formula of degree M, where w_i are their weighting coefficients and χ_i are their knots:

$$c_{mn} = \sqrt{m+\frac{1}{2}} 2^{\frac{-k}{2}} \sum_{i=1}^{M} w_i f\left(\frac{\chi_i + 2n - 1}{2^k}\right) P_m(\chi_i)\, dt \tag{64}$$

The expansion in terms of basic functions can be expressed in vector form in the following way:

$$f(t) = \sum_{n=1}^{2^{k-1}} \sum_{m=0}^{M-1} c_{mn} \psi_{mn}(t) = \bar{C}^t \cdot \bar{\psi}(t) \tag{65}$$

where $\bar{C}$ is a column vector with $M \cdot 2^{k-1}$ elements, grouped in sequences of M elements, formed by the coefficients of expansion. For convenience, it is written in a transposed way:

$$\bar{C}^t = \left(\underbrace{c_{01} c_{11} c_{21} ... c_{M-1,1}}_{M} \underbrace{c_{02} c_{12} c_{22} ... c_{M-1,2}}_{M} ... \underbrace{c_{0,2^{k-1}} c_{1,2^{k-1}} c_{2,2^{k-1}} ... c_{M-1,2^{k-1}}}_{M} \right) \tag{66}$$

On the other hand, $\bar{\psi}(t)$ is also a column vector with $M \cdot 2^{k-1}$ elements, grouped in sequences of M elements, in this case formed by the basic functions of the expansion. Expressed in the form of a row vector:

$$\bar{\psi}^t = \left(\underbrace{\psi_{o1}\psi_{11}\psi_{21}...\psi_{M-1,1}}_{M} \underbrace{\psi_{o2}\psi_{12}\psi_{22}...\psi_{M-1,2}}_{M} ... \underbrace{\psi_{0,2^{k-1}}\psi_{1,2^{k-1}}\psi_{2,2^{k-1}}...\psi_{M-1,2^{k-1}}}_{M} \right) \tag{67}$$

A simple example of wavelet expansion is the Heaviside $u(t)$ function:

$$u(t) = \begin{cases} 0 & t < 0 \\ 1 & t \geq 0 \end{cases} \tag{68}$$

Due to the orthogonality of Legendre polynomials, all coefficients are zero, except all those corresponding to $m = 0$. In vector format, these coefficients are:

$$\bar{G}^t = \frac{1}{2^{\frac{k-1}{2}}} \left(\underbrace{\underbrace{1,0,0,...}_{M}, \underbrace{1,0,0,...}_{M}, ..., \underbrace{1,0,0,...}_{M}}_{2^{k-1}} \right) \tag{69}$$

so $u(t)$ can be expressed:

$$u(t) = \bar{G}^t \cdot \bar{\Psi}(t) \tag{70}$$

If this function is delayed $\frac{1}{2}$, that is, if the function $u\left(t - \frac{1}{2}\right)$ is considered, the first half of the coefficients of its expansion is canceled. Conversely, if it is considered $u(t) - u\left(t - \frac{1}{2}\right)$, the second half is canceled. All this allows to write:

$$u(t) - u\left(t - \frac{1}{2}\right) = \bar{H}^t \cdot \bar{\Psi}(t) \tag{71}$$

where the coefficients $\bar{H}^t$ are:

$$\bar{H}^t = \frac{1}{2^{\frac{k-1}{2}}} \left(\underbrace{\underbrace{1,0,0,...}_{M}, \underbrace{1,0,0,...}_{M}, ..., \underbrace{1,0,0,...}_{M}}_{2^{k-2}} \underbrace{\underbrace{0,0,...}_{M}, \underbrace{0,0,...}_{M}, ..., \underbrace{0,0,...}_{M}}_{2^{k-2}} \right) \tag{72}$$

The basic functions vector $\bar{\psi}(t)$ has the following operational property (see [16]):

$$\int_0^t \bar{\psi}(t')dt' = \bar{\bar{P}} \cdot \bar{\psi}(t) \tag{73}$$

where $\bar{\bar{P}}$ is the integration operational matrix, which has $M \cdot 2^{k-1}$ rows by $M \cdot 2^{k-1}$ columns, block triangular matrix with many zeros. Let's describe it. First, it has a factor $\frac{1}{2^k}$ that multiplies the matrix. On the main diagonal there are 2^{k-1} blocks which are equal tridiagonal matrices of $M \times M$ (it is indicated with $\bar{\bar{L}}$. Above the main diagonal it has equal matrices of $M \times M$ equal to (it is indicated with $\bar{\bar{F}}$). Below the main diagonal there are equal matrices of $M \times M$ formed entirely by zeros ((it is indicated with $\bar{\bar{0}}$). For example, if k = 2 we will have that the matrix $\bar{\bar{P}}$ has the structure:

$$\bar{\bar{P}} = \begin{pmatrix} \bar{\bar{L}} & \bar{\bar{F}} \\ \bar{\bar{0}} & \bar{\bar{L}} \end{pmatrix} \tag{74}$$

Each of these blocks are going to be described now. As discussed above, blocks $\bar{\bar{L}}$ are tridiagonal matrices. The main diagonal is formed by zeros, except for the first element, which is 1, that is, $L_{11} = 1$

if $i = 2.3, ..., M$. The upper diagonal contains $M-1$ elements that are calculated using the expression $(i = 1, 2, ..., M-1)$:

$$L_{i,i+1} = \frac{1}{\sqrt{4i^2-1}} \tag{75}$$

The lower diagonal contains $M-1$ elements that are calculated using the expression $(i = 1, 2, ..., M-1)$:

$$L_{i,i+1} = \frac{-1}{\sqrt{4i^2-1}} \tag{76}$$

On the other hand, blocks $\bar{\bar{F}}$ are made up by zeros, except for $F_{11} = 2$.

4.4. Solving the bioheat equation by Legendre Wavelets

An important application of this operational property is the integration of constant coefficients ordinary linear differential equations systems, like (59) obtained from Bioheat equation (see [13]), which is a first order system. First order equations case is analyzed in detail. In this case, a column vector of functions with N elements is searched. A first order system is represented by the following matrix equations:

$$\begin{aligned} \dot{\bar{x}} &= \bar{\bar{A}} \cdot \bar{x} + \bar{b} \cdot u(t) \\ \bar{x}(0) &= (x_{01}\ x_{02}\ x_{03}\ ...\ x_{0N})^t \end{aligned} \tag{77}$$

where $u(t)$ is the function of Heaviside. In this case, it is looked for a solution of the form $\bar{x}(t) = \bar{\bar{F}}^t \cdot \bar{\Psi}(t)$, where $\bar{\bar{F}}^t$ is an array with N rows and $M \cdot 2^{k-1}$ columns. Remember that $u(t) = \bar{G}^t \cdot \bar{\Psi}(t)$. If these expressions are substituted into the equation (77), we have:

$$\dot{\bar{x}} = \bar{\bar{A}} \cdot \bar{\bar{F}}^t \cdot \bar{\Psi}(t) + \bar{b} \cdot \bar{G}^t \cdot \bar{\Psi}(t) \tag{78}$$

Now, all terms of the above equation are integrated. It's obtained:

$$\int_0^t \dot{\bar{x}} dt' = \int_0^t \bar{\bar{A}} \cdot \bar{\bar{F}}^t \cdot \bar{\Psi}(t') dt' + \int_0^t \bar{b} \cdot \bar{G}^t \cdot \bar{\Psi}(t') dt' \tag{79}$$

If Constants are taken out of each integral, it results:

$$\int_0^t \dot{\bar{x}} dt' = \bar{\bar{A}} \cdot \bar{\bar{F}}^t \cdot \int_0^t \bar{\Psi}(t') dt' + \bar{b} \cdot \bar{G}^t \cdot \int_0^t \bar{\Psi}(t') dt' \tag{80}$$

If equations (73) and $\int_0^t \dot{\bar{x}} dt' = \bar{x} - \bar{x}(0) = \bar{\bar{F}}^t \cdot \bar{\Psi}(t) - \bar{x}(0) \cdot \bar{G}^t \cdot \bar{\Psi}(t)$ are taken into account, It's got:

$$\bar{\bar{F}}^t \cdot \bar{\Psi}(t) - \bar{x}(0) \cdot \bar{G}^t \cdot \bar{\Psi}(t) = \bar{\bar{A}} \cdot \bar{\bar{F}}^t \cdot \bar{\bar{P}} \cdot \Psi(t) + \bar{b} \cdot \bar{G}^t \cdot \bar{\bar{P}} \cdot \Psi(t) \tag{81}$$

If common factor $\bar{\Psi}(t)$ is removed , it is obtained:

$$\bar{\bar{F}}^t - \bar{x}(0) \cdot \bar{G}^t = \bar{\bar{A}} \cdot \bar{\bar{F}}^t \cdot \bar{\bar{P}} + \bar{b} \cdot \bar{G}^t \cdot \bar{\bar{P}} \tag{82}$$

If terms are rearranged, we have:

$$\bar{\bar{F}}^t - \bar{\bar{A}} \cdot \bar{\bar{F}}^t \cdot \bar{\bar{P}} = \bar{b} \cdot \bar{G}^t \cdot \bar{\bar{P}} + \bar{x}(0) \cdot \bar{G}^t \tag{83}$$

If all columns of $\bar{\bar{F}}^t$ are placed one after the other, as a column vector with $N \cdot M \cdot 2^{k-1}$ elements, called $\text{vec}(\bar{\bar{F}}^t)$, and the same is made with the second member of the equation, the previous matrix equation becomes the following linear equations system :

$$\left(\bar{\bar{I}} - \bar{\bar{P}}^t \otimes \bar{\bar{A}}\right) \cdot \text{vec}(\bar{\bar{F}}^t) = \text{vec}(\bar{b} \cdot \bar{G}^t \cdot \bar{\bar{P}} + \bar{x}(0) \cdot \bar{G}^t) \tag{84}$$

where $\bar{\bar{I}}$ is an identity matrix of order $N \cdot M \cdot 2^{k-1}$ and $\bar{\bar{P}}^t \otimes \bar{\bar{A}}$ is the Kronecker product of $\bar{\bar{P}}^t$ i $\bar{\bar{A}}$. It's got a system of $N \cdot M \cdot 2^{k-1}$ equations with $N \cdot M \cdot 2^{k-1}$ unknowns.

It is necessary to remember that a sequence of thermal imaging of a knee has been captured, at the rate of one image every 5 seconds for 20 minutes. It means that the simulation time t ranges from 0 to $t_m = 1200$ s, but Legendre Wavelet ranges from 0 to 1. It is necessary to make a variable change for time t in equation (46), so that the simulation interval is $[0, 1]$ and the discontinuity of q_e is at $t = \frac{1}{2}$. If the new variable is τ, it is defined by:

$$\tau = \frac{t}{t_m} \tag{85}$$

If chain rule is applied for time derivative:

$$\frac{\partial T}{\partial t} = \frac{\partial T}{\partial \tau} \cdot \frac{\partial \tau}{\partial t} = \frac{1}{t_m} \frac{\partial T}{\partial \tau} \tag{86}$$

so equation (46) is converted in:

$$\frac{1}{t_m} \frac{\partial T(z,\tau)}{\partial \tau} = \alpha \frac{\partial^2 T(z,\tau)}{\partial z^2} + \frac{A_o}{\rho c} + \frac{\sigma \left| \vec{E}(z,\tau) \right|^2}{2\rho c} + \frac{T_b - T(z,\tau)}{\tau_b} \tag{87}$$

If this consideration is taken into account and the method of discretization explained above is applied, It's got the following equivalences:

$$\begin{aligned}
\frac{\partial T(z,\tau)}{\partial \tau} &\to \dot{\bar{T}}(\tau) \\
\alpha \frac{\partial^2 T(z,\tau)}{\partial z^2} &\to \alpha \left(\bar{\bar{A}} \bar{T}(\tau) + \bar{\Theta}_a \bar{G}^t \bar{\psi}(\tau) \right) \\
\frac{A_o}{\rho c} &\to \frac{\bar{A}_o \bar{G}^t \bar{\psi}(\tau)}{\rho c} \\
\frac{\sigma \left| \vec{E}(z,\tau) \right|^2}{2\rho c} &\to \bar{q}_e \bar{H}^t \bar{\psi}(\tau) \\
\frac{T_b - T(z,\tau)}{\tau_b} &\to \bar{q}_b \bar{G}^t \bar{\psi}(\tau) - \frac{\bar{T}(\tau)}{\tau_b}
\end{aligned} \tag{88}$$

These equivalences have been made based on what has been discussed in the previous sections, but it is necessary to make some clarifications:

- $\bar{\bar{A}}$ and $\bar{\Theta}_a$: They are expressed as It has been explained in subsection (4.2), equations (54) to (57).
- $\bar{A}_o$ is a constant column vector with its components equal to A_o
- $\bar{q}_e$ and $\bar{e}^t$: Equation (13) can be expressed as:

$$q_e(z,t) = \frac{\sigma \left| \vec{E}_o(z) \right|^2}{2\rho c} \left(u(\tau) - u\left(\tau - \frac{1}{2} \right) \right) \tag{89}$$

where $u(t)$ is the Heaviside function. The factor $\left(u(\tau) - u\left(\tau - \frac{1}{2}\right)\right)$ can be expanded by Legendre Wavelets, using equation (71).It means that the discretization of $q_e(z,\tau)$, that is, a column vector whose components are $q_e(i\Delta z, \tau)$, can be expressed as the product of the column vector $\bar{q}_e$ by the expansion $\bar{G}^t \cdot \bar{\Psi}(t)$, where the components of $\bar{q}_e$ are

$$q_{e,i} = \frac{\sigma \left| \vec{E}_o(i\Delta z) \right|^2}{2\rho c} \tag{90}$$

- $\bar{q}_b$ is a constant column vector with its components all equal to $\frac{T_b}{\tau_b}$
- When the equation (87) is discretized and becomes a system of linear differential equations, $T(z,0)$ becomes a column vector $\bar{T}(0)$, which components are $T(0)_i = T(i\Delta z, 0)$.

A single tissue model is being considered, but a multilayer model, consisting of multiple superimposed layers of tissue (dermis, fat, muscle, etc.) would be more realistic. A first approach to consider is assumption. that the electromagnetic power density is discontinuous in space. In this way, the fact that at different depths the electrical parameters are different would be represented. For example, this proposal is made, with $q_{eo} = 0.015\ \frac{^{\circ}\mathrm{C}}{\mathrm{s}}$:

$$q_e(z)\left[\frac{^{\circ}\mathrm{C}}{\mathrm{s}}\right] = q_{eo}\begin{cases} 1 - 8.67z & z \in [0, 0.0015]\ \mathrm{m}\ \text{(Dermis)} \\ 7.6z + 8.47(0.016 - z) & z \in [0.0015, 0.016]\ \mathrm{m}\ \text{(Fat)} \\ 4.2z + 52(0.036 - z) & z \in [0.016, 0.036]\ \mathrm{m}\ \text{(Muscle)} \\ 3(0.04 - z) & z \in [0.036, 0.04]\ \mathrm{m}\ \text{(Bone)} \end{cases} \tag{91}$$

Under above considerations, Equation (87) is converted in this differential equation system:

$$\frac{\dot{\bar{T}}(\tau)}{t_m} = \alpha\left(\bar{\bar{A}}\bar{T}(\tau) + \bar{\Theta}_a\bar{G}^t\bar{\psi}(\tau)\right) + \frac{\bar{A}_o\bar{G}^t\bar{\psi}(\tau)}{\rho c} + \bar{q}_e\bar{H}^t\bar{\psi}(\tau) + \bar{q}_b\bar{G}^t\bar{\psi}(\tau) - \frac{\bar{T}(\tau)}{\tau_b} \tag{92}$$

which can be transformed as follows:

$$\frac{\dot{\bar{T}}(\tau)}{t_m} = \left(\alpha\bar{\bar{A}} - \frac{\bar{\bar{I}}_{small}}{\tau_b}\right)\bar{T}(\tau) + \left(\alpha\bar{\Theta}_a + \frac{\bar{A}_o}{\rho c} + \bar{q}_b\right)\bar{G}^t\bar{\psi}(\tau) + \bar{q}_e\bar{H}^t\bar{\psi}(\tau) \tag{93}$$

As in the previous section, solutions of the type $\bar{T}(\tau) = \bar{\bar{F}}^t\bar{\psi}(\tau)$ are looked for. Similarly, applying equation ((84)), it's needed to solve this system:

$$\left(\frac{\bar{\bar{I}}_{big}}{t_m} - \bar{\bar{P}}^t \otimes \left(\alpha\bar{\bar{A}} - \frac{\bar{\bar{I}}_{small}}{\tau_b}\right)\right)\mathrm{vec}(\bar{\bar{\mathrm{F}}}^{\mathrm{t}}) = \mathrm{vec}\left(\bar{T}(0)\bar{G}^t + \left(\alpha\bar{\Theta}_a + \frac{\bar{q}_m}{\rho c} + \bar{q}_b\right)\bar{G}^t\bar{\bar{P}} + \bar{q}_e\bar{H}^t\bar{\bar{P}}\right) \tag{94}$$

where $\bar{\bar{I}}_{big}$ is an identity matrix of order $(N-1)\cdot M\cdot 2^{k-1}$, $\bar{\bar{I}}_{small}$ is an identity matrix of order $N-1$.

The simulation of these equations has been performed with the following values of the physical parameters: $\alpha = 1.05\cdot 10^{-7}\ \frac{\mathrm{m}^2}{\mathrm{s}}$, $\tau_b = 800$ s, $q_m = 450\ \frac{\mathrm{W}}{\mathrm{m}^3}$, $h = 22\ \frac{\mathrm{W}}{\mathrm{m}^2\cdot\mathrm{K}}$, $T_a = 23^o$ C and $T_b = 37^o$ C. As it has been said above, $t_m = 1200$ s. After several tests, it has been chosen $k = 3$ and $M = 9$. The result can be seen in figure 7. $T(z,t)$ has been represented at different times. Figure 7.a represents the curves when diathermy is applied, while figure 7.b represents the curves when the system is returning to rest.

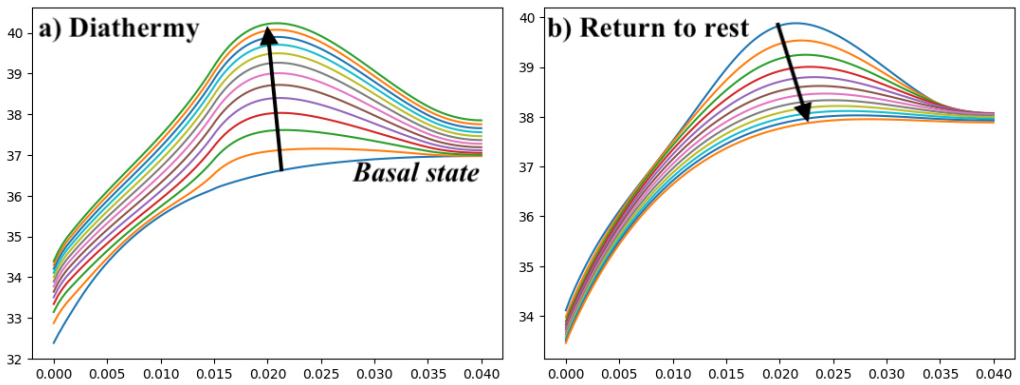

Figure 7. Diathermy application and return to rest curves

5. THE INVERS PROBLEM

It's interesting compare the surface evolution between experimental data and simulation, figure 8 a and b respectively. It's noticeable that qualitative behavior is very similar. Some fine tuning of physical parameters must be done in order to fit this two curves, that can be solved as an **inverse problem**. In order to achieve this goal, some basic concepts are defined.

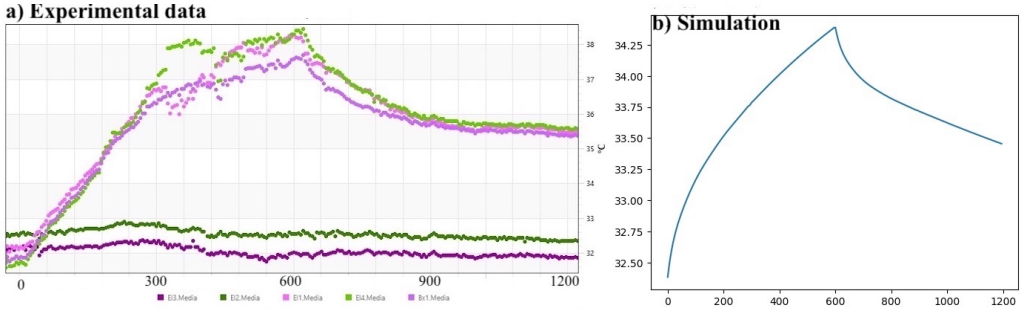

Figure 8. Comparison of surface temperature evolution: a) experimental data; b) simulation

5.1. Basic concepts

The numerical method explained above allows finding the values of the temperature on the surface of the human body at P correlative instants, with time step $\Delta t = 5$ s. These values $T_i = T((i-1)\Delta t)$ with $i = 1, .., P$ can be represented in vector form as $\bar{T}$. This model depends on K parameters p_j, with $j = 1, .., K$, which can be represented too in vector form as $\bar{p}$. Thus, the Bio-heat model can be represented as a function $\bar{T} = f(\bar{p})$ Àt the same correlative instant the temperatures are measured by the thermographic camera. These values $\Theta_i = \Theta((i-1)\Delta t)$, with $i = 1, .., P$, are also represented by a vector $\bar{\Theta}$. If the model was accurate, It would be $\bar{\Theta} = f(\bar{p})$, but actually there is an error in the measurement process, which can be represented by adding a vector term $\bar{\varepsilon}$, that is $\Theta = f(\bar{p}) + \bar{\varepsilon}$. The goal is to determine $\bar{p}$ so that the contribution of $\bar{\varepsilon}$ is as small as possible in the least squares sense, that is, minimization of $||\bar{\varepsilon}(\bar{p})||^2 = \left|\left|\bar{\Theta} - \bar{T}(\bar{p})\right|\right|^2$ by some optimization algorithm. This article proposes an evolutionary algorithm called Evolutionary Centers Algorithm (ECA) [24]. This method will described in the next section. As it is explained in the reference article, the maximization of a function $f(\bar{p})$ is considered, but its application in the case of a minimization is straightforward, making a small transformation to the function.

5.2. Evolutionary Centers Algorithm

It is called **population** a set of parameter vectors, $\Omega = \{\bar{p}_1, \bar{p}_2, \bar{p}_3, \ldots\}$, called **population**. Here a question arises: How does this population change to get a better estimate of the optimal vector? To answer this question, the strategy of analyzing whether each vector in the population can be changed by a new vector is used. To achieve this, for each vector $\bar{p}_i$ of the population, a **sample** of the population, $U = \{\bar{p}_{i_1}, \bar{p}_{i_2}, \bar{p}_{i_3}, \ldots\}$, is randomly selected, and from this sample its "mass center" is calculated. What does it mean? The contribution to the "mass" of the sample of the vector $\bar{u} \in U$ is $f(\bar{p})$, so it can be written:

$$\bar{c}_i = \frac{\sum_{\bar{u}\varepsilon U} f(\bar{u}) \cdot \bar{u}}{\sum_{\bar{u}\varepsilon U} f(\bar{u})} \tag{95}$$

This point tends to approach where there is more "mass concentration", that is, where $f(\bar{p})$ has larger values. It would be an estimate of where the maximum is located. In order to get closer to the solution, a random element of the sample, $\bar{u}_r \in U$, is selected, from which the **candidate** $\bar{t}_i$ is:

$$\bar{t}_i = \bar{p}_i + \eta \cdot (\bar{c} - \bar{u}_r) \tag{96}$$

where η is a random number between 0 and η_{max}. If $f(\bar{t}_i) > f(\bar{p}_i)$, then $\bar{p}_i$ is changed by $\bar{t}_i$ into the population, which is updated. Otherwise, the population remains unchanged.

6. RESULTS AND CONCLUSIONS

Equation (19) has been simulated using the method described in Section 4. The programming language used to carry out the computations has been ***Julia*** programming language [1], into a Jupyter Notebook IDE. In order to test this method, the model has been simulated with the following values:

$$\alpha = 1.19 \cdot 10^{-7} \ \frac{\mathrm{m}^2}{\mathrm{s}}, \tau_{\mathrm{b}} = 1000 \ \mathrm{s}, \mathrm{q}_{\mathrm{eo}} = 0.0150 \ \frac{^{\mathrm{o}}\mathrm{C}}{\mathrm{s}} \tag{97}$$

The evolution of surface temperatures has been found, and Gaussian noise has been added, with zero-average and standard deviation $s = 0.13$ ^{o}C. The ECA algorithm has been applied with bounds:

$$\alpha \in [0, 10^{-6}], \tau_b \in [100, 2000], q_e \in [0.007, 0.030] \tag{98}$$

In the Figure 9 can be seen the simulated and identified data and the difference between simulated data without noise and identified data. It's noticeable the little difference among them. The identified parameters that have been obtained and its percent relative errors are shown below:

$$\alpha = 1.28 \cdot 10^{-7} \ \frac{\mathrm{m}^2}{\mathrm{s}}, \tau_{\mathrm{b}} = 913 \ \mathrm{s}, \mathrm{q}_{\mathrm{eo}} = 0.0155 \ \frac{^{\mathrm{o}}\mathrm{C}}{\mathrm{s}} \tag{99}$$

$$\frac{\Delta\alpha}{\alpha} = 7.6\%, \frac{\Delta\tau_b}{\tau_b} = 8.7\%, \frac{\Delta q_{eo}}{q_{eo}} = 3.3\% \tag{100}$$

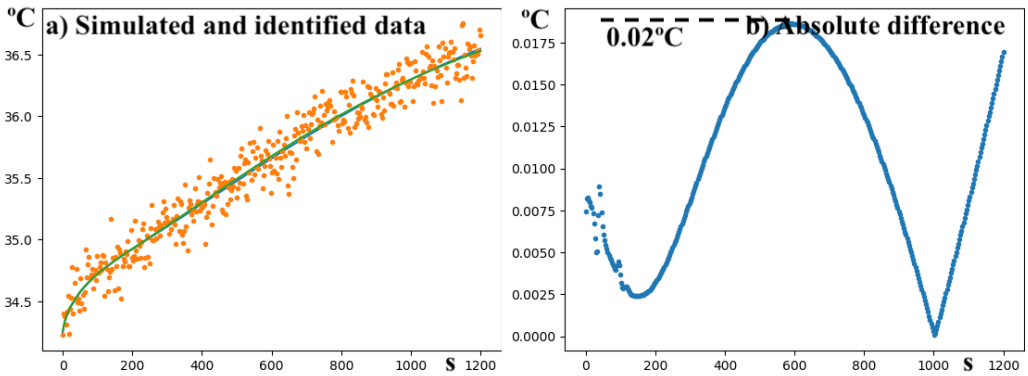

Figure 9. Comparison of simulated and identified data

These results are quite promising, since an acceptable identification of three parameters has been obtained from a single temperature curve. the number of variables can be modified to analyze how the uncertainty in the results is changed. Moreover, this technique can be assessed in other contexts and compared with other techniques commonly used to solve inverse problems, such as regularization techniques [26].

References

[1] Pennes, H.H. (1948). Analysis of tissue and arterial blood temperatures in the resting human forearm. Journal of Applied Physiology, 1, 93-122.
[2] Cattaneo, M.C. (1958). A form of heat conduction equation which eliminates the paradox of instantaneous propagation. Compte Rendus, 247, 431-433.
[3] Vernotte, P. (1958). Les paradoxes de la theorie continue de l'equation de la chaleur. Compte Rendus, 246, 3154-3155.
[4] Tzou, D.Y. (1996). Macro- to Microscale Heat Transfer: The Lagging Behavior. Washington, DC: Taylor and Francis.
[5] Cao, K and Lesnic, D. (2018). Reconstruction of the perfusion coefficient from temperature measurements using the conjugate gradient method. International Journal of Computer Mathematics, 95 (4). pp. 797-814.

[6] J Iljaž and L C Wrobel and T Gomboc and M Hriberšek and J Marn. (2020). Solving inverse bioheat problems of skin tumour identification by dynamic thermography. Inverse Problems IOP Publishing. Volum 36 Number 3
[7] Luna, José Manuel, Hernández Guerrero, Abel, Romero Méndez, Ricardo, Luviano Ortiz, José Luis. (2014). Solution of the Inverse Bio-Heat Transfer Problem for a Simplified Dermatological Application: Case of Skin Cancer. Ingeniería mecánica, tecnología y desarrollo, 4(6), 219-228.
[8] Marek Rojczyk, Helcio R.B. Orlande, Marcelo J. Colaço, Ireneusz Szczygieł, Andrzej J. Nowak, Ryszard A. Białecki, Ziemowit Ostrowski (2015), Inverse heat transfer problems: an application to bioheat transfer. Computer Assisted Methods in Engineering and Science, 22: 365–383.
[9] Antonio Marcio Gonçalo Filho and Lucas Lagoa Nogueira and Joao Victor Caetano Silveira and Michelli Marlane Silva Loureiro and Felipe dos Santos Loureiro. (2017). Solution of the Inverse Bioheat Transfer Problem for the Detection of Tumors by Genetic Algorithms, ICCSA.
[10] Ramo, Simon and Whinnery, John and Duzer, Theodore. (1994). Fields and Waves In Communication Electronics.
[11] IT'IS Foundation. Tissues properties database. https://www.itis.ethz.ch/virtual-population/tissue-properties/database/dielectric-properties/
[12] Bezanson, Jeff and Edelman, Alan and Karpinski, Stefan and Shah, Viral B. Julia: A fresh approach to numerical computing. SIAM review. Vol 59. Pages 65-98.
[13] George B. Arfken, Hans J. Weber. (1995). Mathematical Methods for Physicists (Fourth Edition), Academic Press. Pages 693-765
[14] Milton Abramowitz. (1974). Handbook of Mathematical Functions, With Formulas, Graphs, and Mathematical Tables. Dover Publications, Inc., USA.
[15] Polikar, Robi. (1999). The story of wavelets. 192-197.
[16] Razzaghi, Mohsen and Yousefi, Samira. (2001). The Legendre wavelets operational matrix of integration. International Journal of Systems Science. 32. 495-502.
[17] Venkatesh, S.G. and Ayyaswamy, S.K. and Balachandar, Sivaramakrishnan. (2012). The Legendre wavelet method for solving initial value problems of Bratu-type. COMPUTERS AND MATHEMATICS WITH APPLICATIONS. 63. 1287-1295.
[18] Venkatesh, S.G. and Ayyaswamy, S.K. and Balachandar, Sivaramakrishnan. (2012). Convergence analysis of Legendre wavelets method for solving Fredholm integral equations. Applied Mathematical Sciences (Ruse).
[19] Gümgüm, Sevin and Ozdek, Demet and Özaltun, Gökçe. (2019). Legendre Wavelet Solution of High Order Nonlinear Ordinary Delay Differential Equations. Turkish Journal of Mathematics.
[20] Vanani, S. and Hafshejani, J and Sadeghi, Mahmoud. (2011). Numerical Solution of Delay Differential Equations Using Legendre Wavelet Method. World Applied Sciences Journal. 13. 27-33.
[21] Balaji, S.. (2014). Legendre Wavelet Operational Matrix Method for Solution of Riccati Differential Equation. Journal of the Egyptian Mathematical Society.
[22] Kumar, Dinesh and Kumar, Pappu and Rai, Kavindra. (2017). Numerical solution of non-linear dual-phase-lag bioheat transfer equation within skin tissues. Mathematical Biosciences.
[23] Dutta, Jaideep and Kundu, Balaram. (2017). A revised approach for an exact analytical solution for thermal response in biological tissues significant in therapeutic treatments. Journal of Thermal Biology. 66. 33-48.
[24] J.-A. Mejía-de-Dios, E. Mezura-Montes. (2019). A New Evolutionary Optimization Method Based on Center of Mass, In Decision Science in Action: Theory and Applications of Modern Decision Analytic Optimisation, editors, Kusum Deep, Madhu Jain, Said Salhi, 65–74. Springer Singapore, Singapore.
[25] McIntosh, Robert L. and Anderson, Vitas. (2010). A comprehensive tissue properties database provided for the thermal assessment of a humant at rest, Biophysical Reviews and Letters. Volume 5, number 3, pages 129-151.
[26] A.N. Tikhonov, V.Y. Arsenin. (1977) Solutions of Ill-Posed Problems. V.H. Winston and Sons. Washington, D.C.